 doi:10.20944/preprints202210.0324.v1

Article

Shaking Table Testing of Reinforced Concrete IMRF Structure

Sida Hussain[1], Hamna Shakeel[1], Asif Ali[1], Muhammad Rizwan[2] and Naveed Ahmad[3,*]

[1] Deparmtment of Civil Engineering, UET Peshawar, 25000 Khyber Pakhtunkhwa, Pakistan
[2] Deparmtment of Civil Engineering, SUIT Peshawar, 25000 Khyber Pakhtunkhwa, Pakistan
[3] Deparmtment of Civil and Environmental Engineering, Stanford University, 94305 CA, USA
*Corresponding author: drnaveed@stanford.edu

Abstract: Multi-level shaking table tests were performed on 1:3 reduced scale two-story RC IMRF frames conforming to ACI-318-19. The exterior joints lacked shear reinforcement to assess the viability of the ACI model recommended for determining the design shear strength of the beam-column joint panel. The Northridge-1994 earthquake accelerogram was input to the frame for multi-level shaking table testing. Plastic hinges developed in beams under base input motion with a maximum acceleration equal to 0.40g. The exterior joints incurred extensive damage under base input motion with a maximum acceleration equal to 0.70g. The frame achieved displacement ductility and overstrength factors equal to 2.40 and 2.50 respectively. This gives a response modification factor equal to 6. The satisfactory performance of the frame is attributed to the high efficiency of the beam-column joint, which was confined by spandrel beams on two faces, and the high strength of the concrete. The inherent minimal confinement is sufficient to ensure good seismic behavior. The analysis confirmed overstrength equal to 1.58 for joint shear strength in comparison to the design strength determined using the ACI model. The data might serve as a reference for calibrating and validating numerical modeling techniques for performance evaluation, which are crucial in the context of performance-based engineering.

Keywords: joint shear capacity; ACI-318-19; ductility factor; IMRF; reinforced concrete

1. Introduction

A ductile frame exhibits reduced lateral stiffness and increased energy dissipation that tends to reduce seismic forces relative to forces that would occur in a linearly elastic frame[1,2,3]. Therefore, such frame can be designed for lower seismic forces given in seismic code ASCE/SEI-7-16[4]. It is achievable if frames are properly detailed to attain such ductile behaviour. Therefore, the IBC-2018[5] relies primarily on the ACI-318-19[6] Code that list design procedures and minimum requirements for ductile detailing. The structural frame members are intended to resist design basis earthquake motion through ductile response but without critical deteriorations of strength.

The ASCE/SEI-7-16 permits the use of intermediate moment-resisting frame (IMRF) as a lateral load-resisting system for structures assigned to seismic design category (SDC) B and C. The code suggests it may also be permitted as part of dual systems for structures assigned to SDC D, E, and F. In this case, the IMRF is designed for a portion of lateral load (e.g. 25% of total base shear) but intended to deform in congruence with the dual system. The SDC assigned to a structure depends on the intended use and occupancy of the building and the ground motions at the site. The IBC-2018[5] suggests the building should be assigned to the more severe SDC.

Based on the observations from past experimental tests performed on interior and exterior beam-column sub-assemblages[7], the ACI-318-19 recommends transverse reinforcement in beam-column joints unless the joint is restrained on all four sides by beams. The joint transverse reinforcement is intended to confine the joint concrete and preclude longitudinal column bars buckling. This requirement is relieved when the beam framing in to the joint extends from the opposite face of the joint up to the length at least equal to

Preprints (www.preprints.org) | NOT PEER-REVIEWED | Posted: 21 October 2022 doi:10.20944/preprints202210.0324.v1

the beam depth[8], and also ensuring the extending beam/column members are properly dimensioned and reinforced to provide effective restraints to joint.

The present research confirms through series of shake-table tests performed on a two-story IMRF that if the exterior beam-column joint is confined by appropriately detailed spandrel beams on two faces and the joint concrete has compressive strength equal to/greater than 4000 psi (28 MPa), the joint efficiency will improve. The frame achieved strength and toughness sufficient to resist design basis earthquake ground motions without deterioration of strength. The selected frame was tested progressively till the joint capacity was fully exhausted and the frame was found in the near collapse state. The joint efficiency was quantified that was compared with the joint shear strength obtained using the ACI model given in the ACI-318-19 to assess the efficacy of the design strength model for considered frame.

The ACI-318-19 suggests the exterior beam-column joints of the intermediate moment-resisting frame shall have transverse reinforcements that are distributed within the column height equal to the beam depth. This shear reinforcement is based on the requirements of ACI-352R[9], and intends to prevent deterioration due to shear cracking and buckling of longitudinal column reinforcement. The present research confirms through shake-table tests that such stringent requirements may be relaxed especially for low-rise intermediate moment-resisting frames when the exterior joints are confined by beams on three faces and concrete has compressive strength equal to or more than 4000 psi (28 MPa). The inherent minimal joint confinement is sufficient to ensure good seismic behavior.

2. Design of selected moment-resisting frame

Lateral Seismic Forces

The selected frame is a two-story one-bay moment-resisting frame (**Fig. 1**). The preliminary member sizes chosen and material properties considered for the frame are reported in **Table 1**. The seismic base shear force V for the frame was computed in accordance with the equivalent lateral force procedure given in the ASCE/SEI-7-16:

$$V = C_S W \tag{1}$$

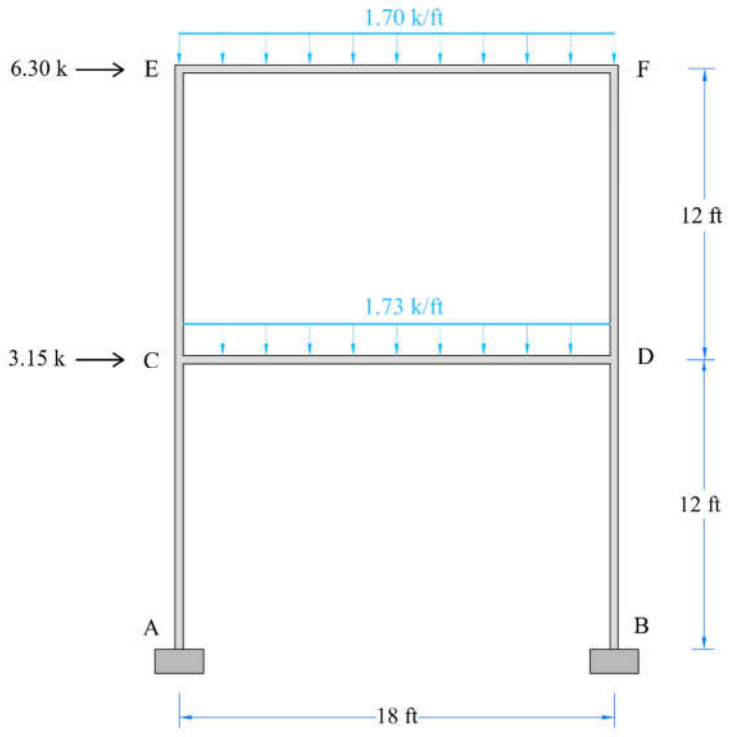

Figure 1. Selected moment-resisting reinforced concrete frame.

Preprints (www.preprints.org) | NOT PEER-REVIEWED | Posted: 21 October 2022 doi:10.20944/preprints202210.0324.v1

Table 1. Preliminary chosen sizes of beams and columns, and basic material properties.

Member	Depth in. (mm)	Width in. (mm)	Clear Span in. (mm)	f_c' ksi (MPa)	E_c ksi (GPa)	f_y ksi (MPa)	E_s ksi (GPa)
Beams:	18 (457)	12 (305)	204 (5182)	4 (28)	3605 (24.86)	60 (414)	29000 (200)
Columns:	12 (305)	12 (305)	138 (3505)	4 (28)	3605 (24.86)	60 (414)	29000 (200)

The value of seismic response coefficient C_S depends on a number of geotechnical and seismic characteristics of the site and the type of structural system used to resist lateral seismic forces. **Table 2** reports the values considered for selected frame. The value of C_S was determined in accordance with the procedure given in ASCE/SEI-7-16 (12.8.1.1). The response modification coefficient R needs attention, as this accounts for reduction of the design spectral response acceleration for ductile structures capable of dissipating seismic energy through inelastic deformation in hinging regions of members. The ASCE/SEI-7-16 recommends R to be taken 5.0 for intermediate moment-resisting frame. Moreover, the selected frame was assigned to SDC C with earthquake importance factor I_e equal to 1.25. The Rayleigh method and eigenvalue analysis of elastic frame model provide accurate estimate of fundamental time period of structures[10]. However, the fundamental time period of frame T = 0.42 sec was computed in accordance with the empirical equation suggested in ASCE/SEI-7-16 (12.8.2.1), which is based on the earlier work of Goel and Chopra[11,12], that provides a conservative estimate of the seismic response coefficient. The upper limit coefficient C_u was taken 1.5 in accordance with the ASCE/SEI-7-16 for selected design spectral response acceleration parameter. This gives seismic response coefficient C_S equal to 0.118, which was increased by 30 percent (i.e. $C_S = 1.3 \times 0.118 \approx 0.15$) in accordance with the orthogonal seismic loads combination procedure proposed in the ASCE/SEI-7-16 (C12.5.3) based on the earlier work of Veletsos and Newmark[13]. The design base shear force V was approximated equal to 9.54 kips (42.42 kN). The lateral seismic force F_x = [6.30 kips (28 kN), 3.15 kips (14 kN)] for roof and first-floor respectively were computed in accordance with the vertical distribution factor C_{vx} given in ASCE/SEI (12.8.3).

Table 2. Geotechnical, seismic and structural parameters considered for design of frame.

SDC	S_{DS}	S_{D1}	*Soil*	I_e	R	Ω_0	C_d
C	0.5	0.2	B	1.25	5.0	3	4.5

Design of Beams

The beams were designed for flexure and shear actions in accordance with the ACI-318 (18.4.2). The design of beams was based on the demands for beam member CD, since it will be subjected to higher bending and shears actions. **Fig. 2** shows the factored design moment M_{ub} for combined gravity and lateral seismic forces. Positive bending-moments are plotted below the beam centroid and negative moments are plotted above the centroid. The ACI-318 recommends the beam shall have at least two continuous longitudinal bars at both top and bottom faces. For this reason, and to simplify the construction of test frame, three longitudinal steel bars 3#6 (i.e. diameter equal to 19 mm) were selected for both top/bottom faces of beam. The nominal moment strength M_{nb} of selected doubly reinforced beam section was calculated through an iterative procedure as described by Wight[14]. For the materials properties given in **Table 1**, a value of M_{nb} = 98 k-ft (133 kN-m) and the reduced nominal moment strength ϕM_{nb} equal to 88 k-ft (120 kN-m) were determined. The demand-to-capacity ratio of the selected beam is 0.85 that gives a flexural overstrength equal to 1.17. This indicates the appropriateness of the selected tension reinforcement for top face of beam. Under lateral seismic loads reversal, the reinforcement in the bottom face of beam will develop similar flexural strength in tension.

Preprints (www.preprints.org) | NOT PEER-REVIEWED | Posted: 21 October 2022 doi:10.20944/preprints202210.0324.v1

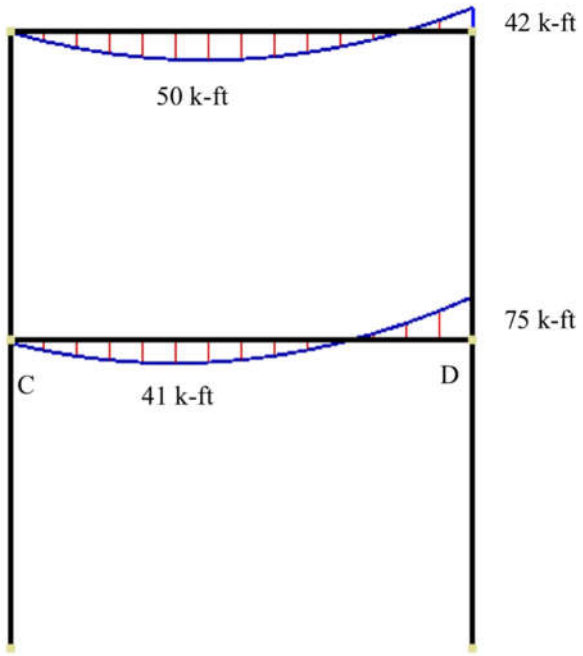

Figure 2. Factored design moment M_{ub} for beams for combined gravity and lateral seismic forces.

The factored shear force was computed in accordance with the ACI-318-19 (18.4.2.3) that suggests two procedures for determining shear: a) based on the free body diagram and assuming that nominal moment strengths (taking $\phi = 1$) are developed at both ends of the beam and, b) analyzing the frame for lateral seismic forces including the earthquake effects doubled i.e. 2*E*. In present case, procedure (a) gives value 7% higher than procedure (b). **Fig. 3** shows the considered factored design shear V_{ub} for combined gravity and lateral seismic forces.

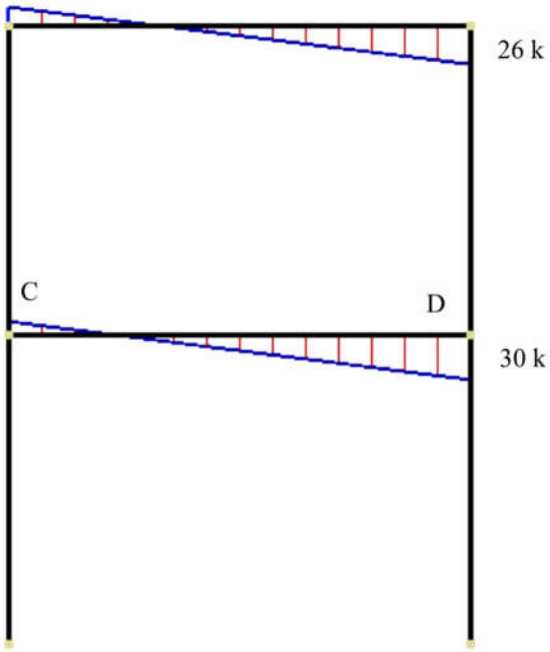

Figure 3. Factored design shear V_{ub} for beams in accordance with ASCE/SEI-7-16 (18.4.2.3).

The nominal shear strength V_{nb} was calculated in accordance with the ACI-318-19 (22.5.1) for one-way shear. In comparison with the classical model for shear strength of concrete V_{cb}[15], the updated models now include also the effects of member depth and

Preprints (www.preprints.org) | NOT PEER-REVIEWED | Posted: 21 October 2022 doi:10.20944/preprints202210.0324.v1

longitudinal reinforcement ratio on shear strength[16,17]. This is due to the fact that the beams with increased depth and reduced area of longitudinal reinforcement exhibit lower shear stress at failure[18,19,20,21]. The updated model gives value equal to 10.85 kips (48.26 kN) for reduced nominal shear strength of concrete ϕV_{cb}. This was found 31% less than the previous simple model[16]. The shear reinforcement was computed in accordance with the ACI-318-19 (22.5.8.5.3). In the present case #3 (diameter equal to 9.53 mm) double-legs stirrups were used as shear reinforcement and taking the longitudinal spacing s of the shear reinforcement equal to 3 in. (76 mm). The demand-to-capacity ratio computed for shear reinforcement is 0.55. The section still maintains demand-to-capacity ratio equal to 0.72, even if the concrete component is ignored. This gives shear overstrength equal to 1.40. Moreover, the appropriateness of the selected cross-sectional dimensions was also checked in accordance with the ACI-318-19 (22.5.1.2) that gives demand-to-capacity ratio of 0.42, indicating the efficacy of the selected sizes of beam cross-section. The designed shear reinforcement also conforms to the provisions of ACI-318-19 (18.4.2.4).

Design of Columns

The beams of frame are designed as yielding members while columns and beam-column joints are capacity-protected through appropriate dimensions and detailing. This intends to ensure strong-column and weak-beam lateral load-resisting frame for seismic energy dissipation without compromising the stability of frame[22]. However, the additional requirement of ACI-318-19 (18.7.3.2) that recommends flexural strengths of the special moment resisting columns shall satisfy the criteria $\sum M_{nc} \geq (6/5)\sum M_{nb}$ is compromised for intermediate moment-resisting frames; the factor (6/5) may be taken equal to 1. Therefore, factored moment M_{uc} for columns were computed for the design base combined gravity and lateral seismic forces (**Fig. 4**). The design of columns was based on the member BD, since ground story columns are subjected to higher combined actions (moment, axial, shear and story-drift). The column design moments were further increased to take in to account the flexural overstrength of beam (i.e. 1.17). A value of 47 ft-k (64 kN-m) and 44 k (196 kN) were obtained for design moment M_{uc} and the corresponding axial force P_{uc} respectively.

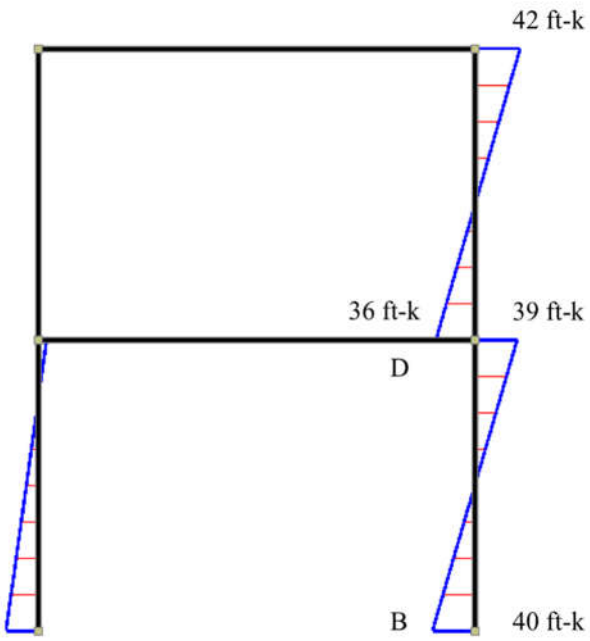

Figure 4. Factored design moment M_{uc} for columns for combined gravity and lateral seismic forces.

Preprints (www.preprints.org) | NOT PEER-REVIEWED | Posted: 21 October 2022 doi:10.20944/preprints202210.0324.v1

The selected columns were assumed with 8#6 (diameter 19 mm) longitudinal bars. Likewise, the nominal moment strength M_{nc} of selected column section was calculated through an iterative procedure as described by Wight[14]. For the materials properties given in **Table 1**, a value of M_{nc} = 60 k-ft (81 kN-m) and the reduced nominal moment strength ϕM_{nc} equal to 54 k-ft (73 kN-m) were determined for tension-controlled section with pre-compression P_{uc}. The demand-to-capacity ratio of the selected column is 0.87 that gives a flexural overstrength equal to 1.15. This indicates the appropriateness of the selected reinforcement for the column section.

The factored shear force for column was computed in accordance with the ACI-318-19 (18.4.3.1) that suggests procedures similar to ACI-318-19 (18.4.2.3) for beam shear. However, the earthquake effect E is increased by overstrength factor Ω_0 equal to 3.0. **Fig. 5** shows the factored design shear force for columns. Likewise, the nominal shear strength V_{nc} was calculated in accordance with the ACI-318-19 (22.5.1). Similarly, #3 (diameter equal to 9.53 mm) double-legs stirrups were used as shear reinforcement of columns and taking the longitudinal spacing s equal to 3 in. (76 mm). The demand-to-capacity ratio computed for shear reinforcement is equal to 0.33, and it is equal to 0.40 if the concrete component is ignored. This gives shear overstrength equal to 2.50 and confirms the appropriateness of the selected shear reinforcement.

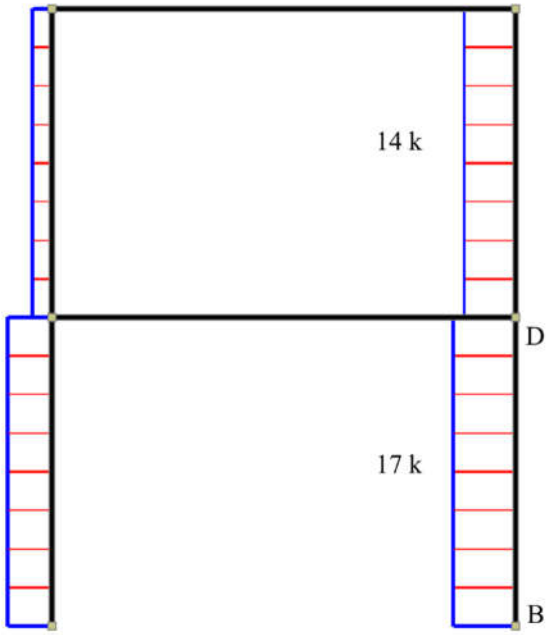

Figure 5. Factored design shear V_{uc} for columns for combined gravity and lateral seismic forces.

Design of Beam-Column Joints

The beam-column joints of test frame were confined on all three faces: a main beam resisting in-plane loads and two transverse beams of similar sizes and reinforcement. Design of joint C is discussed. The joint shear $V_{u,joint}$ was computed in accordance with the ACI-318-19 (18.4.4.7.1). This requires horizontal shear force on a plane at mid-height of the joint $V_{u,joint}$ to be calculated using Equation (2) and (3)[14]:

$$V_{u,joint} = T_{pr} - V_{col} \tag{2}$$

$$T_{pr} = \alpha A_S f_y \tag{3}$$

Moreover, the ACI-318-19 suggests using tensile and compressive beam forces and column shear consistent with beam nominal moment strength M_{nb}. Therefore parameter α is taken equal to 1.0. The tensile force T_{pr} is found equal to 80 kips (356 kN). For M_{nb} = 98

Preprints (www.preprints.org) | NOT PEER-REVIEWED | Posted: 21 October 2022 doi:10.20944/preprints202210.0324.v1

k-ft (133 kN-m), V_{col} is found equal to 70 kips (311 kN). The nominal joint shear strength $V_{n,joint}$ was computed in accordance with the ACI-318-19 (18.8.4.3) using Equation (4):

$$V_{n,joint} = 15\lambda\sqrt{f_c'}A_j \tag{4}$$

The modification factor λ is taken equal to 1.0 for normal concrete. The joint area A_j is taken equal to 144 in² (92903 mm²). The value of $V_{n,joint}$ is found equal to 137 kips (610 kN). This gives reduced nominal joint shear strength $\phi V_{n,joint}$ equal to 82 kips (366 kN). The demand-to-capacity ratio was found equal to 0.86, indicating joint shear overstrength equal to 1.17 for design base actions. This shows the efficacy of the considered joint laterally supported by beams on three faces. In the present research, the shake table tests will also confirm the efficiency of the considered joint. **Fig. 6** shows the reinforcement details of the selected beam/column members and beam-column joint panel for test frames.

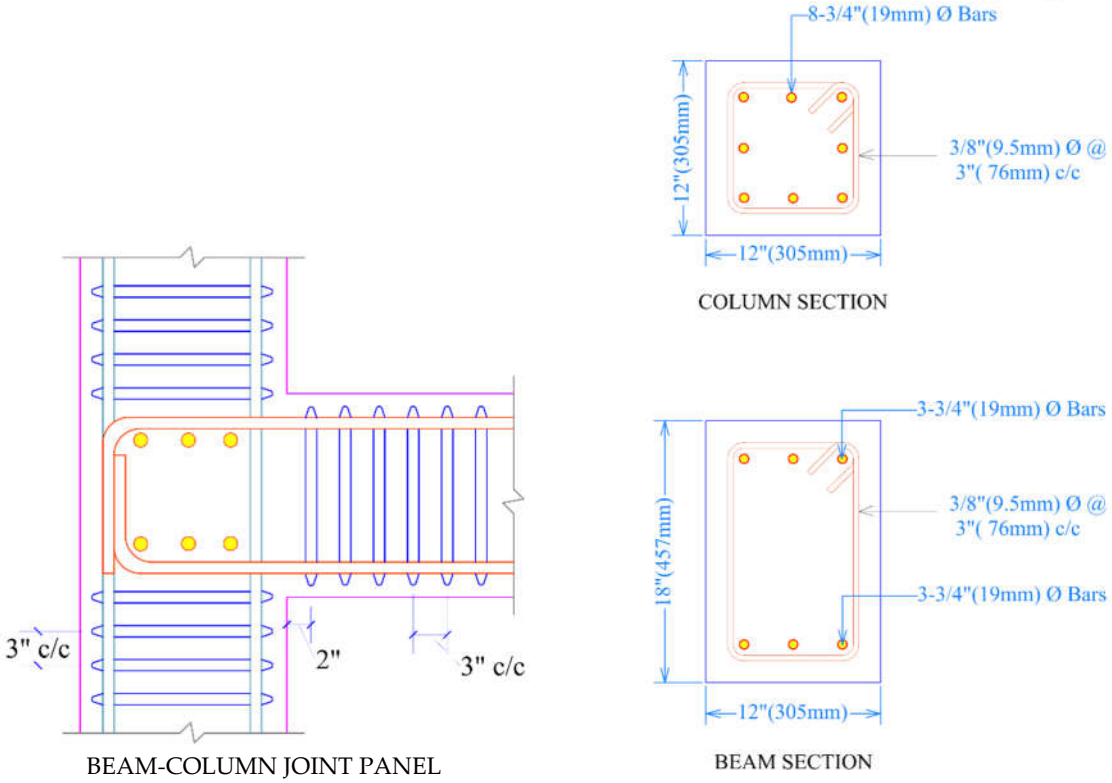

Figure 6. Geometric and reinforcement details of the beam/column members and panel.

3. Shake-table tests on selected frame

Fig. 7 shows the 1:3 reduce-scaled test frame prepared using the similitude requirements for a simple model. The linear dimensions of beam/column members, slab and diameter of reinforcement were reduced by a scale factor S_L = 3. The concrete used constituents in a mix proportion as 1:1.68:1.72 (cement: sand: aggregate) with water-to-cement weight equal to 0.48, in order to achieve the required compressive strength of concrete. The test frame model was also provisioned with additional floor mass M_{mf} in accordance with the similitude requirements for dynamic seismic analysis of model described in Moncarz and Krawinkler[23]:

$$M_r = \frac{M_p}{M_m} = S_L^2 \tag{5}$$

$$M_{mf} = \frac{M_{p1}}{S_L^2} - M_{m0} \tag{6}$$

Preprints (www.preprints.org) | NOT PEER-REVIEWED | Posted: 21 October 2022 doi:10.20944/preprints202210.0324.v1

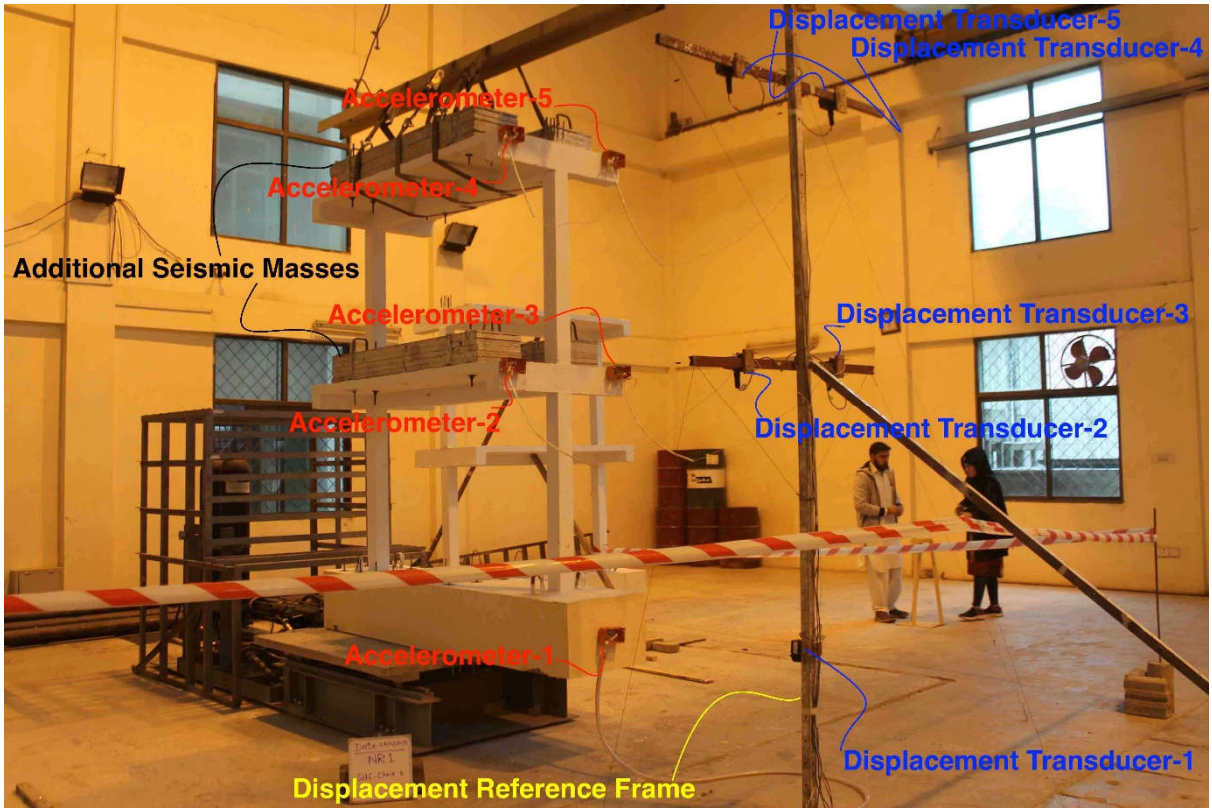

Figure 7. A 1:3 reduced scale test frame.

An additional floor mass equal to 1.33 kips (5.90 kN) was applied on each floor using steel blocks of 300 kg on each side of the main beam. The weights were placed outside the effective width of beam. Two displacement string pots and two accelerometers were mounted at the mid-height of the slab at each floor level on transverse beams, in order to measure response histories of floor displacements and floor accelerations. One string pot and accelerometer were also mounted at the base of the model to measure the actual input base motions.

The acceleration time history of Northridge-1994 earthquake was selected for input base motions. This was recorded at CASTAIC OLD RIDGE RT, 090 CDMG STATION 24278. **Fig. 8** shows the design response spectrum for parameters given in **Table 2** and the scaled acceleration response spectrum of selected accelerogram. The scaling is performed by linearly matching the spectral accelerations of accelerogram and the design spectrum at the fundamental time period of frame (T = 0.42 sec). Moreover, the accelerogram was time-compressed by a factor of $S_L^{1/2} = 3^{1/2}$ to satisfy the similitude requirement[24] for base motion of 1:3 reduced scale test frame.

Preprints (www.preprints.org) | NOT PEER-REVIEWED | Posted: 21 October 2022 doi:10.20944/preprints202210.0324.v1

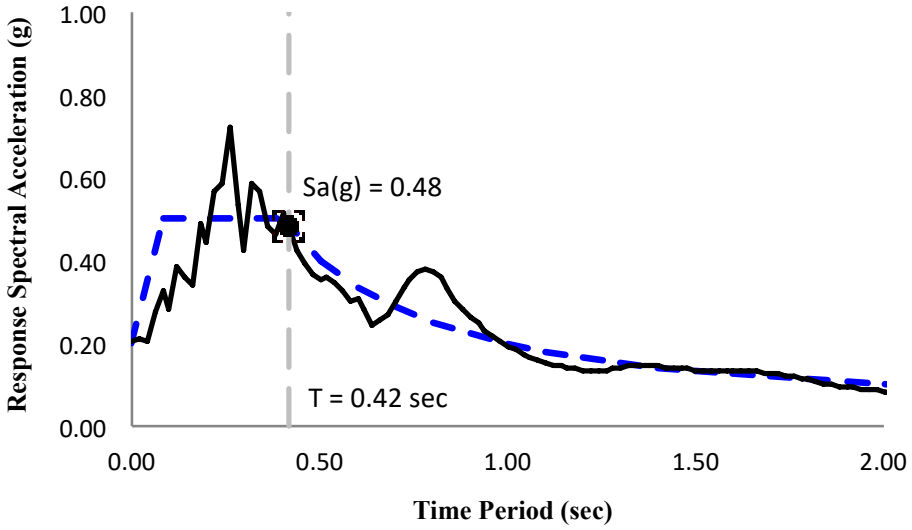

Figure 8. Scaled acceleration response spectrum of Northridge-1994 for base motions.

Table 3 reports the values of measured sustained maximum accelerations at the base of models for series of test runs. The observed damages in each test are also reported in **Table 3** and shown in **Fig. 9** through **Fig. 11**. The test frame exhibited horizontal and vertical flexural cracks at the beam-joint interface, which aggravated with increasing amplitude of base motions. The beam-column joint panels incurred extensive damages under base motions with sustained maximum acceleration equal to 0.70g.

Table 3. Measured sustained maximum acceleration of base motions of test frame.

Test Runs	PHA* (g)	Remarks
1	0.20	-
2	0.40	Horizontal and vertical flexural cracks at the beam-joint interface.
3	0.45	Aggravation of horizontal flexural cracks at the beam ends. Occurrence of slight cracks in beam-column joints
4	0.70	Extensive damages occurred at the beam-column joint panels on both floor levels.

*Peak horizontal acceleration

Preprints (www.preprints.org) | NOT PEER-REVIEWED | Posted: 21 October 2022 doi:10.20944/preprints202210.0324.v1

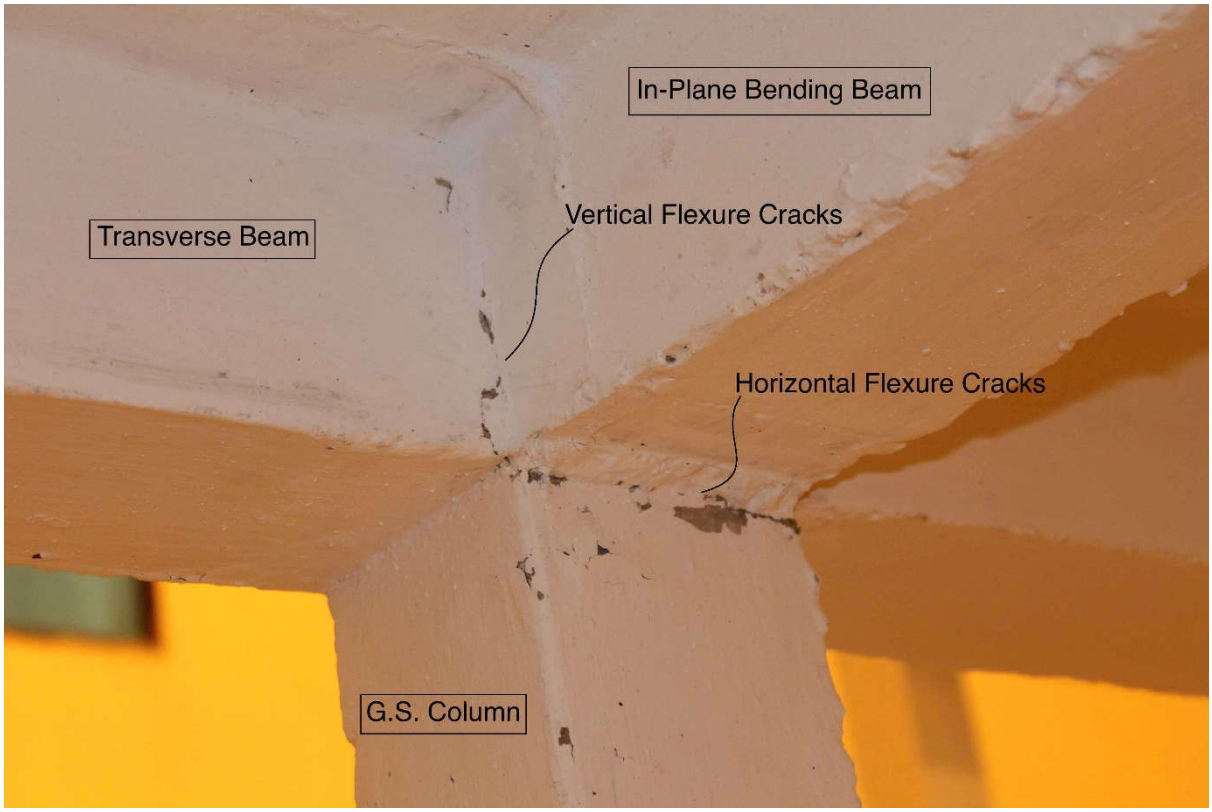

Figure 9. Horizontal and vertical flexural cracks at the beam-joint interface under test run 2 (ref. Table 3).

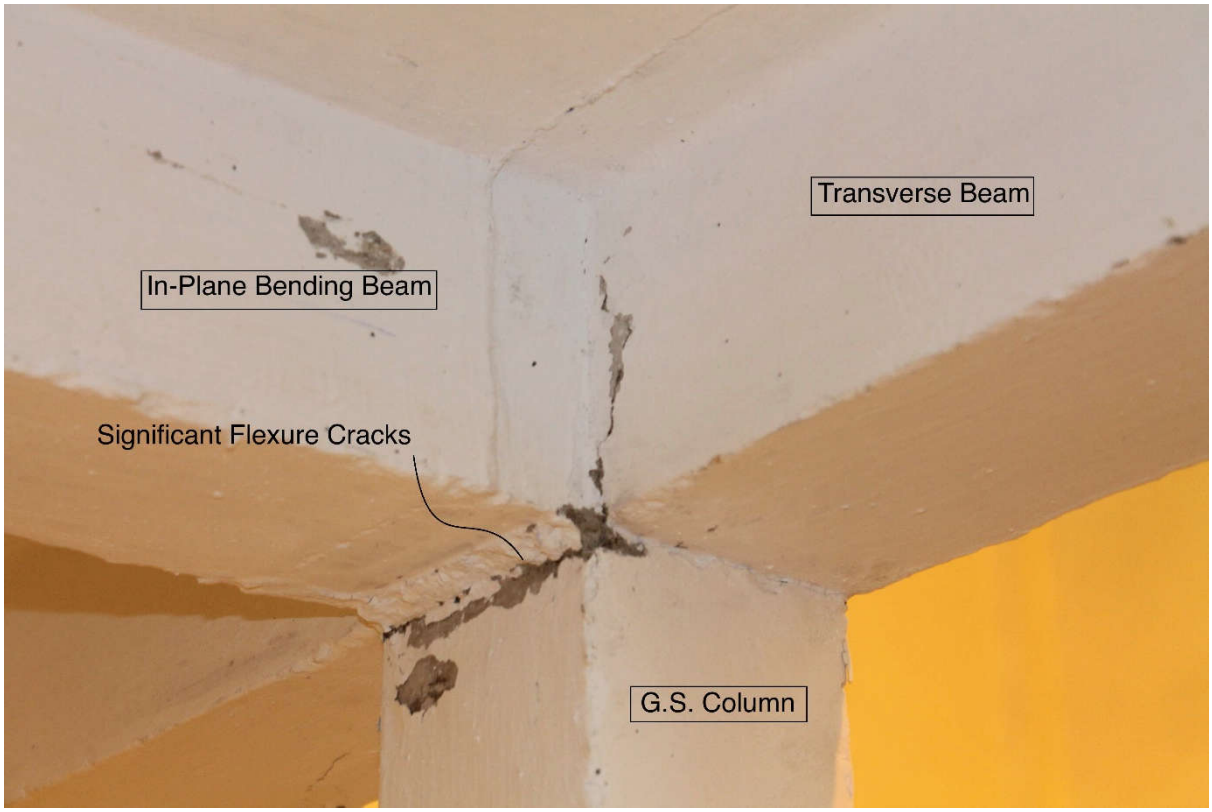

Figure 10. Aggravation of horizontal flexural cracks at the beam ends under test run 3 (ref. Table 3).

Preprints (www.preprints.org) | NOT PEER-REVIEWED | Posted: 21 October 2022 doi:10.20944/preprints202210.0324.v1

Figure 11. Extensive damage occurred at beam-column joint panel under test run 4 (ref. Table 3).

4. Seismic design factors for selected frame

Overstrength Factor

The beam/column members of selected frame were designed with capacities greater than the design forces. It is most likely the actual materials strength is higher than the nominal strength specified in the design. Moreover, the test frame also comprised the slab that acts monolithically with the beam. These sources are likely to increase the actual maximum lateral strength (V_{max}) of frame in comparison to the design lateral strength (V). The ratio of the V_{max} to V is referred to as overstrength factor Ω_o. The ASCE/SEI-7-16 suggests Ω_o equal to 3 for IMRF.

The measured response histories of floor accelerations and displacements for all test runs were processed to compute the relative displacement of roof and the corresponding base shear force for prototype of test frame. The first three runs were analyzed to develop force-displacement capacity curve for the prototype of tested frame (**Fig. 12**). The capacity curve exhibits hardening response in the post-yield state. The ASCE/SEI 7-116(12.12) suggests the allowable story drift equal to $0.020h_{sx}$ for the selected frame that was considered as the maximum drift for computing the peak base shear force. A value equal to 23.83 kips (106 kN) is obtained. This gives overstrength factor equal to 2.50, which is 20% less than the value suggested by ASCE/SEI-7-16 for selected frame.

Preprints (www.preprints.org) | NOT PEER-REVIEWED | Posted: 21 October 2022 doi:10.20944/preprints202210.0324.v1

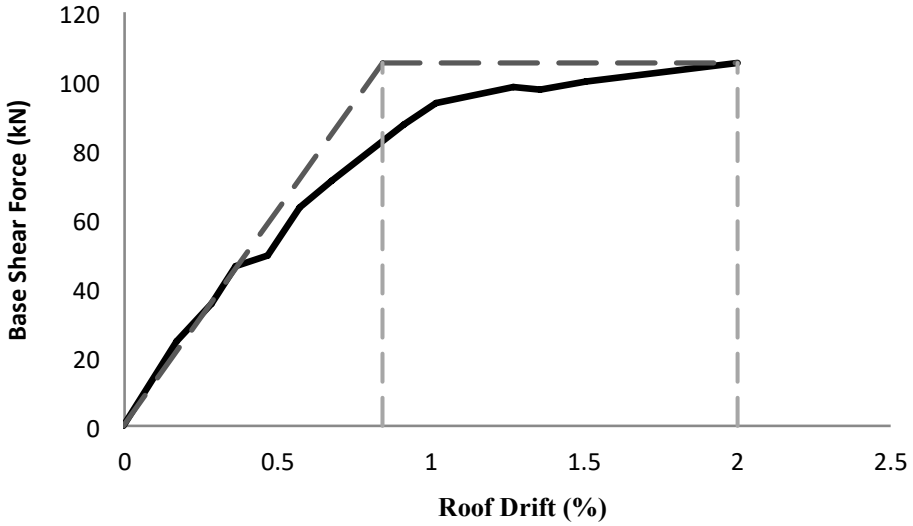

Figure 12. Force-displacement capacity curve for prototype of tested frame.

Fig. 13 shows the considered plastic mechanism of selected frame for analytical prediction of peak base shear force. The virtual work method was used to compute V_{max} using Equation (7) and (8):

$$W_{ve} = W_{vi} \tag{7}$$

$$0.835V_{\max} = \theta\left(4M_{pb} + 2M_{pc}\right) \tag{8}$$

For M_{pb} = 98 k-ft (133 kN-m), M_{pc} = 60 k-ft (81 kN-m) and θ = 1/24 rad (1/7.315 rad), V_{max} equal to 25.54 kips (113.62 kN) is obtained. This gives an overstrength factor equal to 2.68, which is approximately 11% less than the value suggested by ASCE/SEI-7-16 and 7.20% higher than the value obtained using the experimental force-displacement curve. This confirms the efficacy of the analytical method for computing the peak base shear force at the maximum permissible drift.

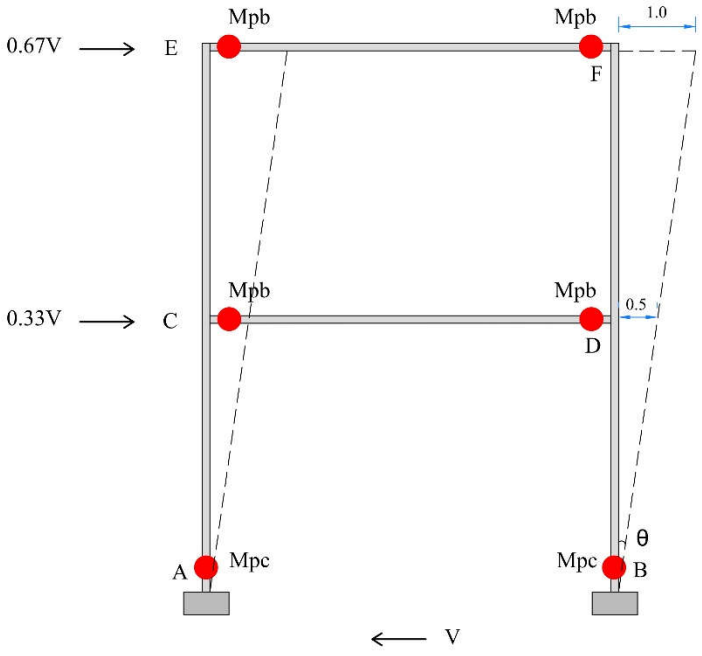

Figure 13. Considered plastic mechanism of selected frame.

Preprints (www.preprints.org) | NOT PEER-REVIEWED | Posted: 21 October 2022 doi:10.20944/preprints202210.0324.v1

Ductility Factor

The ductility factor of a structure is a measure of its global nonlinear response, which is related to the global displacement ductility of structure[25]. The global effective yield displacement Δ_y was obtained using the FEMA-P695 procedure[26]. Considering the allowable story drift equal to $0.020h_{sx}$ as the maximum permissible drift, the displacement ductility ratio μ was found equal to 2.40 ($\mu = \Delta_{max}/\Delta_y \approx 2.40$). The bi-linearized capacity curve gives yield time period T_y of frame equal to 0.72 sec for the first mode of vibration assuming linear deflected shape, which is greater than 0.50 sec. Thus, the ductility factor R_μ is taken equal to displacement ductility ratio i.e. $R_\mu = \mu = 2.40$ in accordance with the suggestion of Newmark and Hall[26] for SDOF system with elasto-plastic nonlinear response.

Alternatively, the effective yield displacement was computed in accordance with the suggestion of Priestley et al[27] in order to assess efficacy of the analytical prediction. The yield drift of a story for reinforced concrete frame is computed using Equation (9):

$$\theta_y = 0.5\varepsilon_y \frac{L_b}{h_b} \tag{9}$$

For $\varepsilon_y = 0.0021$, $L_b = 18$ ft (5486 mm) and $h_b = 18$ in. (457 mm) the yield drift was found equal to 1.24. It is sufficiently accurate to approximate the global effective yield drift of frame equal to story drift for a linear deflected shape of frame under lateral seismic forces. This gives displacement ductility ratio equal to 1.61, which is 33% less than the ductility ratio obtained based on the experimental global nonlinear response curve. This significant difference is due to the fact that the analytical model given in Equation (9) is based on the response of beam-column connection sub-assemblages that did not include slab. Nevertheless, this analytical model is conservative for design purposes.

Response Modification Coefficient

This factor is used to calculate the seismic response coefficient required for determination of seismic base shear using the equivalent lateral force procedure given in the ASCE 7-16 for seismic design of structure. For a structure, the response modification coefficient R is described as the product of the overstrength factor Ω_o and the ductility factor R_μ i.e. $R = \Omega_o \times R_\mu$. The experimental data gives R equal to 6.0 ($R = 2.50 \times 2.40 = 6.0$), which is 20% higher than the value suggested in the ASCE 7-16 for selected frame (i.e. $R = 5$). This increase is due to the higher ductility capacity of tested frame.

The analytical predictions based on the virtual work method for computation of peak base shear and the empirical formula suggested by Priestley et al for computation of effective yield displacement gives R equal to 4.31 ($R = 2.68 \times 1.61 = 4.31$), which is 28% less in comparison to the R factor obtained using the experimental data. The analytically computed R factor (i.e. 4.31) is approximately 14% less than the value suggested in the ASCE 7-16. This confirms the analytical models give conservative value for response modification coefficient.

5. Assessment of Beam-Column Joint

Efficiency of Beam-Column Joint

The efficiency of a joint is the measure of its reserve strength. For a connection, this is computed as the ratio of the force causing failure of the joint to the force corresponding to the moment capacity of the yielding beam entering the joint. For a global structure, the efficiency of the considered beam-column joint, which is laterally supported by beams on three faces, was determined by computing ratio of the base shear force causing failure of the joint V_f to the base shear force (V_{max}) developed at the maximum permissible drift under design base earthquake (**Fig. 14**). This gives efficiency of joint equal to 1.56 or 156%. The measured efficiency is significantly higher than the values reported for typical corner joints subjected to bending causing opening of the joint[28,29]. This is due to the fact the considered beam-column joint was laterally supported by beams on two faces in addition to the in-plane beam entering the joint. Moreover, the corresponding roof deflection capacity

Preprints (www.preprints.org) | NOT PEER-REVIEWED | Posted: 21 October 2022 doi:10.20944/preprints202210.0324.v1

was found equal to 4.70%, which is 135% higher than the maximum permissible drift under design base earthquake. Considering the maximum considered earthquake (MCE) ground motions equal to 3/2 times of the design base earthquake (DBE) ground motions, the measured roof drift capacity is 57% higher than the permissible drift under MCE ground motions. This confirms the available sufficient reserve strength and high efficiency of the beam-column joint confined by beams on three faces (**Fig. 6**) despite the fact it lacks shear reinforcement.

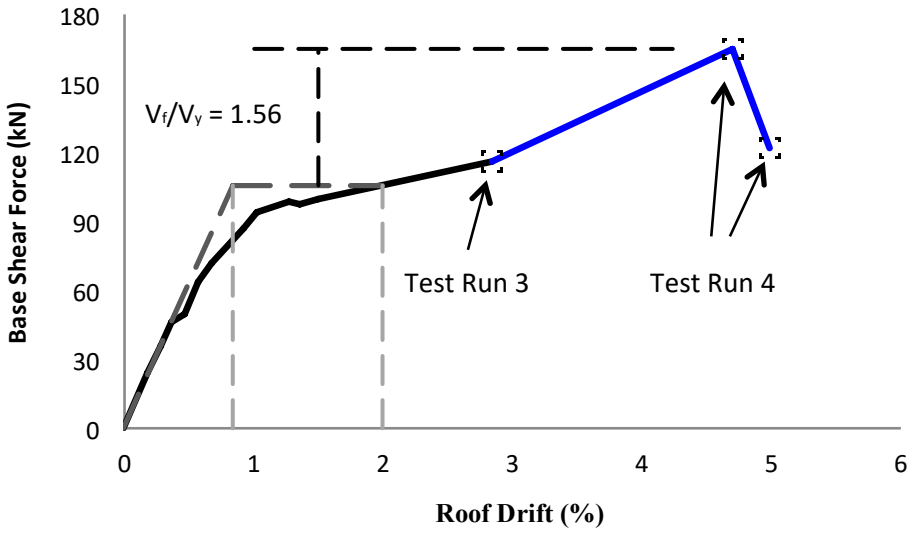

Figure 14. Complete capacity curve for prototype of tested frame till beam-column joints were extensively damaged. .

Shear Strength of Beam-Column Joint

Joint C of frame was analyzed for determination of joint shear strength. For test run 4, the corresponding floor forces at the peak base shear (**Fig. 14**) were obtained. This gives $F_{x,f}$ = [24.28 kips (108 kN) 12.14 kips (54 kN)] for roof and first-floor respectively. The corresponding story shear forces V_S = [12.14 kips (54 kN) 18.21 kips (81 kN)]] were obtained for column CE and AC respectively. This gives bending moments at the joint M_c = [72.28 k-ft (98 kN-m) 108.42 k-ft (147 kN-m)]] for column CE (at the base end) and column AC (at the top end) respectively. The point of contraflexure is assumed at the mid-height of the column for computing moments at the column end. The equilibrium of bending moments at the joint will require the bending moment in beam equal to 181.44 k-ft (246 kN-m). This gives flexural overstrength of beam equal to 1.85 in comparison to nominal bending moment capacity of beam. This increase is attributed to the materials overstrength and slab contribution to flexural strength of beam, as suggested earlier by French and Moehle[30]. This develops a maximum tension force $T_{pr,max}$ in the joint equal to 147.92 kips (658 kN). The corresponding maximum joint shear force $V_{u,joint,max}$ was found equal to 129.71 kips (577 kN) using Equation (2) and the experimentally obtained story shear and joint tensile force. This gives overstrength equal to 1.58 for joint shear strength in comparison to nominal shear strength determined in accordance with the ACI-318-19 (18.8.4.3). This confirms the efficacy of the considered beam-column joint (**Fig. 6**) of selected frame despite the fact it lacks shear reinforcement. However, concrete must have a compressive strength equal to or more than 4000 psi (28 MPa) for such good behavior.

6. Conclusions

Summary

Based on the preliminary design of selected frame, the following conclusions are drawn:

 doi:10.20944/preprints202210.0324.v1

1. The analysis of beam indicates overstrength equal to 1.17 for flexural strength and 1.40 for shear strength. The corresponding flexural and shear overstrength obtained for column are 1.15 and 2.50 respectively.
2. The factored shear force computed in accordance with the ACI-318-19 provisions 18.4.2.3 (a) and 18.4.2.3 (b) gives roughly similar shear force with procedure (a) gives relatively high shear force by 7% in comparison to procedure (b).
3. The updated model for shear strength of concrete included in ACI-318-19 gives strength 31% less than the previous simple model.
4. The analytical model gives overstrength equal to 1.17 for shear capacity of joint for design base actions. This confirms the efficacy of the joint laterally supported by beams on three faces despite the facts it lacks shear reinforcement. However, it must be ensure that the concrete has compressive strength equal to or more than 4000 psi (28 MPa).

Conclusions

Based on the observed seismic performance of selected moment-resisting frame under series of shake-table tests, the following conclusions are drawn:

1. The selected frame exhibited flexural mechanism in beams under base motions with sustained maximum acceleration up to 0.40g. Only few slight cracks were developed in beam-column joints under base motions with sustained maximum acceleration equal to 0.45g. The joints incurred extensive damage under base motion with sustained maximum acceleration of 0.70g.
2. The selected frame achieved overstrength factor equal to 2.50, which is 20% less than the value suggested by ASCE/SEI-7-16. The ductility factor was found equal to 2.40, which is 44% higher than the ductility factor inherently available in the response modification coefficient suggested by ASCE/SEI-7-16 for selected frame. This gives response modification coefficient equal to 6.0, which is 20% higher than the value suggested by ASCE/SEI-7-16.
3. The available analytical model for yield drift provided estimate of ductility factor 33% less than the experimental value. It is due to the fact that such models are based on response of beam-column connection sub-assemblages lacking slab effects.
4. The virtual work method based on the presumed plastic mechanism predicted the peak base shear of selected frame at roof drift of 2% with sufficient accuracy; slightly overestimated by 7%. However, this method underestimated the maximum resistance of frame at roof drift of 4.20% by 31%. This is due to the fact that the method ignored the material overstrength and slab contribution to flexural strength. Re-calculating V_{max} using Equation (8) and amplifying bending moment capacity of beam by flexural overstrength of 1.85 gives Vmax equal to 42.26 kips (188 kN). This is approximately 14% higher than the experimentally observed maximum resistance of 37.10 kips (165 kN).
5. The efficiency of joint that defines the ratio of force causing failure of the joint to the force developed in the structure at the maximum permissible drift was found equal to 1.56 (or 156%). This measured efficiency is significantly higher than the values reported previously[28,29]. This increase is attributed to the material overstrength and the fact that the joint was confined by beams on three faces and the concrete strength is 4000 psi (28 MPa).
6. Analysis of joint based on experimental response at the roof drift equal to 4.70% gives overstrength equal to 1.58 for joint shear strength in comparison to nominal shear strength determined in accordance with the ACI-318-19 (18.8.4.3). The measured high overstrength confirms the efficacy of the beam-column joint confined by beams on three faces despite the fact it lacks shear reinforcement. However, it is a must to use

 doi:10.20944/preprints202210.0324.v1

concrete that has compressive strength equal to or more than 4000 psi (28 MPa). The inherent minimal confinement is sufficient to ensure good seismic behavior.

Acknowledgments: The authors are grateful to the Board of Advanced Studies and Research (BOASAR) of UET Peshawar for financing the experimental part of the present research work and similar ongoing research projects of postgraduate students.

Conflicts of Interest: The authors declare that they have no known financial conflicts of interest or close personal relationships that may have seemed to have influenced the research described in this study.

Notation:

A_j = joint area

A_S = area of longitudinal steel reinforcement in tension

C_d = deflection amplification factor

C_S = seismic response coefficient

C_u = coefficient for upper limit on fundamental time period, 1.5 for S_{D1} equal to 0.20

C_{vx} = Vertical distribution factor

E = effect of earthquake-induced forces

E_c = Young's modulus of concrete

E_s = Young's modulus of steel

F_x = lateral seismic design forces at level x

$F_{x,f}$ = lateral seismic forces at level x at lateral force causing failure of the joint

$f_c^{'}$ = compressive strength of concrete

f_y = yield strength of steel

g = acceleration due to gravity equal to 32.17 ft/s^2 (9.81 m/s^2)

h_b = depth of beam

h_{sx} = story height below level x

I_e = earthquake importance factor based on the use and occupancy of the structure

L_b = length of beam

M_{m0} = floor mass of test model

 doi:10.20944/preprints202210.0324.v1

M_{mf} = additional floor mass for test model

M_n = nominal moment strength

M_{p1} = floor mass of prototype of test model

M_{pb} = plastic moment of beam section

M_{pc} = plastic moment of column section

M_r = prototype-to-model mass ratio

M_u = factored design moment

P_u = factored axial load

R = response modification coefficient

R_μ = ductility factor

S_{DS} = design spectral response acceleration parameter in the short period range

S_{D1} = design spectral response acceleration parameter for stuctural period equal to 1.0 sec

S_L = scale factor

T = fundamental period of the structure

T_{pr} = tensile force in longitudnal reinforcement of beam in tension

V = design lateral strength, design base shear force

V_c = shear strength of concrete

V_{col} = column shear force

V_f = peak lateral force causing failure of the joint

$V_{\max}$ = maximum lateral strength, up to permissble maximum design drift

V_n = nominal shear strength

V_S = story shear force

V_u = factored shear force

 doi:10.20944/preprints202210.0324.v1

$V_{n,joint}$ = nominal shear strength of joint

$V_{u,joint}$ = factored shear strength of joint

W = effective seismic weight of structure

W_{ve} = virtual external work

W_{vi} = virtual internal work

Δ_y = effective yield displacement

Δ_{max} = maximum displacement corresponding to maximum permissible design drift

ε_y = strain of steel correspodning to yield stress

μ = displacement ductility ratio

Ω_0 = overstrength factor

ϕ = strength reduction factor

θ = story drift

θ_y = effective yield drift

References

1. Gulkan, P., and Sozen, M. A., "Inelastic response of reinforced concrete structures to earthquake motions," *ACI Structural Journal*, V. 89, No. 1, Jan.-Feb. 1974, pp. 89-98.
2. Blume, J. A., Newmark, N. M., and Corning, L. H., "Design of multistory reinforced concrete buildings for earthquake motions," Portland Cement Association, Skokie, IL, 1961, 318 pp.
3. Park, R., and Paulay, T., "Reinforced concrete structures", Wiley – Interscience, New York, 1975, 768 pp.
4. ASCE/SEI 7-16 "Minimum design loads and associated criteria for buildings and other structures," American Society of Civil Engineers, Reston, Virginia, 2017, 822 pp.
5. IBC-2018 "International Building Code," International Code Council, Washington, D.C. 2019, 726 pp.
6. ACI-318-19 "Building code requirements for structural concrete," American Concrete Institute, Farmington Hills, MI, 2019, 822 pp.
7. Hanson, N. W., and Connor, H. W., "Seismic resistance of reinforced concrete beam-column joints," *Journal of the Structural Division* ASCE, V. 93, No. ST5. Oct. 1967, pp. 533-560.
8. Meinheit, D. F., and Jirsa, J. O., "Shear strength of reinforced concrete beam-column joints," Report No. 77-1, Department of Civil Engineering, Structures Research Laboratory, University of Texas at Austin, Austin, TX, Jan. 1977, 291 pp.
9. ACI 352R-02 "Recommendation for design of beam-column connections in monolithic reinforced concrete structures – ACI-ASCE Committee 352," American Concrete Institute, Farmington Hills, MI, 2019, 822 pp.
10. Chopra, K. A., "Dynamics of structures, theory and applications to earthquake engineering - 4th Ed.," Prentice Hall, Upper Saddle River, NJ, 2012.
11. Goel, R. K., and Chopra, A. K., "Period formulas for moment-resisting frame buildings," *Journal of Structural Engineering ASCE*, V. 123, No. 11, 1997 pp. 1454-1461.
12. Goel, R. K., and Chopra, A. K., "Period formulas for concrete shear wall buildings." *Journal of Structural Engineering ASCE*, V. 124, No. 4, 1998, pp. 426-433.
13. Rosenblueth, E., and Contreras, H., "Approximate design for multicomponent earthquakes," *Journal of Engineering Mechanics Division ASCE*, V. 103, No. 5, 1977, pp. 881-893.
14. Wight, J. K., "Reinforced concrete: mechanics and design - 7th Ed.," Pearson Education Inc., Hoboken, NJ, 2016, 1144 pp.
15. MacGregor, J. G., and Hanson, J. M., "Proposed changes in shear provisions for reinforced and pre-stressed concrete beams," *ACI Journal Proceedings*, V. 66, No. 4, Apr. 1969, pp. 276-288.

16. Kuchma, D., Wei, S., Sanders, D., Belarbi, A., and Novak, L., "The development of the one-way shear design provisions of ACI 318-19," *ACI Structural Journal*, V. 116, No. 4, July 2019.
17. Sneed, L. H., and Ramirez, J., "Influence of effective depth on the shear strength of concrete beams – experimental study", *ACI Structural Journal*, V. 107, No. 5, Sept., 2010, pp. 554-562.
18. Bazant, Z. P., Yu, Q., Gerstle, W., Hanson, J., and Ju, J., "Justification of ACI 446 code provisions for shear design of reinforced concrete beams," *ACI Structural Journal*, V. 104, No. 5, Sept.-Oct., 2007, pp. 601-610.
19. Angelakos, D., Bentz, E. C., and Collins, M. D., "Shear strength of large members," *ACI Structural Journal*, V. 98, No. 3, May-June, 2001, pp. 290-300.
20. Lubell, A. S., Sherwood, E. G., Bentz, E. C., and Collins, M. P., "Safe shear design of large wide beams," *Concrete International*, V. 26, No. 1, Jan., 2004, pp. 66-78.
21. Brown, M. D., Bayrak, O., and Jirsa, J. O., "Design for shear based on loading conditions," *ACI Structural Journal*, V. 103, No. 4, July-Aug., 2006, pp. 541-550.
22. Sozen, M. A., "Seismic behavior of reinforced concrete buildings," *Earthquake Engineering*, Y. Bozorgnia and V. V. Bertero, ed., CRC Press, New York, 2004, pp. 13-1 to 13-41.
23. Moncarz, P., and Krawinkler, H., "Theory and application of experimental model analysis in earthquake engineering," Report No. 50, Department of Civil and Environmental Engineering, John Blume Earthquake Engineering Center, Stanford University, Stanford, CA, June 1981, 263 pp.
24. El-Attar, A-G., White, R. N., and Gergely, P., "Shake table test of a 1/6 scale two-story lightly reinforced concrete building," Report No. 50, Department of Civil and Environmental Engineering, National Center for Earthquake Engineering Research, State University of New York at Buffalo, NY, February 1991, 263 pp.
25. Newmark, N. M., and Hall, W. J., "Earthquake spectra and design," Earthquake Engineering Research Institute, Oakland, CA, August 1982, 103 pp.
26. FEMA-P-695 "Quantification of building seismic performance factors," Federal Emergency Management Agency (FEMA), Washington, DC, June 2009, 421 pp.
27. Priestley, M. J. N., Calvi, G. M., and Kowalsky, M. J., "Displacement based seismic design of structures," IUSS Press, Pavia, 2007 721 pp.
28. Nilsson, I. H. E., and Losberg, A., "Reinforced concrete corners and joints subjected to bending moment," Proceedings ASCE, Journal of the Structural Division, Vol. 102, No. ST6, June 1976, pp. 1229-1254.
29. Balint, P.S., and Taylor, H. P. J., "Reinforcement detailing of frame corner joints with particular reference to opening corners," Technical Report, Cement and Concrete Association, London, February, 1972, 16 pp.
30. French, C. W., and Moehle, J. P., "Effect of floor slab on behaviour of slab-beam-column connections, *Design of Beam-Column Joints for Seismic Resistance*, SP-123, American Concrete Institute, Farmington Hills, 1991, pp.225-258.